Adiabatic dynamics of a quantum critical system coupled to an environment: Scaling and kinetic equation approaches

Dario Patanè and Luigi Amico
Dipartimento di Metodologie Fisiche e Chimiche (DMFCI) and MATIS CNR-INFM, Università di Catania, viale A. Doria 6, 95125 Catania, Italy and Departamento de Física de Materiales, Universidad Complutense, 28040 Madrid, Spain

Alessandro Silva
The Abdus Salam International Centre for Theoretical Physics, Strada Costiera 11, 34100 Trieste, Italy

Rosario Fazio
NEST-CNR-INFM and Scuola Normale Superiore, Piazza dei Cavalieri 7, I-56126 Pisa, Italy

Giuseppe E. Santoro
International School for Advanced Studies (SISSA), Via Beirut 2-4, 34014 Trieste, Italy;
CNR-INFM Democritos National Simulation Center, Via Beirut 2-4, 34014 Trieste, Italy;
and The Abdus Salam International Centre for Theoretical Physics, Strada Costiera 11, 34100 Trieste, Italy
(Received 21 December 2008; revised manuscript received 7 May 2009; published 2 July 2009)

We study the dynamics of open quantum many-body systems driven across a critical point by quenching a parameter of the Hamiltonian at a certain velocity. General scaling laws are derived for the density of excitations and of energy produced during the quench as a function of the quench velocity and the bath temperature. The scaling laws and their regimes of validity are verified for the *XY* spin chain locally coupled to bosonic baths. A detailed derivation and analysis of the kinetic equations for the problem is presented.

DOI: 10.1103/PhysRevB.80.024302 PACS number(s): 64.60.Ht, 64.70.Tg, 03.65.Yz

I. INTRODUCTION

A series of beautiful experiments on the dynamics of cold atomic gases[1–3] spurred renewed interest in the study of nonequilibrium quantum many-body systems. On the theoretical side, these experiments triggered an intense investigation mostly devoted to the simplest paradigm of nonequilibrium quantum dynamics; the controlled variation in time of one of the system parameters (quantum quenches). In the case of sudden quenches, where the driving parameter is changed on a time scale much shorter than the typical time scales of the system, a number of important issues have been addressed. We mention, for example, the study of the signatures of universality in the quench dynamics of quantum critical systems,[4] the presence of thermalization in integrable vs nonintegrable systems,[5] as well as the description of generic nonequilibrium quenches using thermodynamic variables[6] and their statistics.[7]

In this paper we will focus on the opposite case in which the control parameter is varied *adiabatically*. This situation becomes particularly interesting when a quantum critical point is crossed during the adiabatic evolution. Indeed the vanishing of the energy gap at the critical point makes the system unable to follow adiabatically the driving remaining in its equilibrium/ground state no matter how slow is the quench. The study of this deviation from the adiabatic dynamics is a very important problem in a number of different branches of physics ranging from the defect formation in the early universe[8,9] to adiabatic quantum computation[10] and quantum annealing.[11,12] Depending on the context, the loss of adiabaticity has been characterized by the excess energy at the end of the quench, by the density of defects (if the final state is a fully ordered system), or by the fidelity of the time evolved state with respect to the ground state of the Hamiltonian at the end of the quench.

The scaling of the density of excitations generated during the dynamics as a function of the velocity of the quench was first predicted for a quantum critical system in Refs. 13 and 14. The mechanism behind the generation of excitations/defects is similar to the so-called Kibble-Zurek (KZ) mechanism[8] first proposed for classical phase transitions. Following these initial works a number of specific models were scrutinized[15–29] thereby confirming the general picture.

All the studies mentioned previously assumed unitary Hamiltonian dynamics. When this condition is lifted we face the problem of understanding the effect of an external environment on the adiabatic dynamics of open quantum critical systems. This issue is of paramount importance in several contexts, for example, in the case of adiabatic quantum computation, decoherence is a fundamental limiting factor for the implementation of quantum algorithms. Decoherence is in turn always present as a result of the unavoidable coupling of any system to an environment. As a result of this, even the experimental verification of the KZ scaling in a quantum critical system at low velocities will sooner or later see the presence of the thermostat. Despite its importance, the adiabatic dynamics of open critical systems is a much less studied problem. The effect of classical and quantum noise acting uniformly on a quantum Ising chain was considered in Refs. 30 and 31, respectively. Numerical simulations for a model of local noise on a disordered Ising model were performed in Ref. 32. Moreover, the effect of a static spin bath locally coupled to an ordered Ising model is studied in Ref. 33. In a recent Letter,[34] we have addressed the universality of the

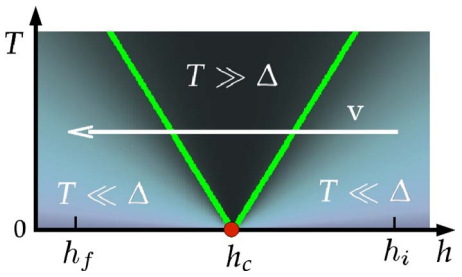

FIG. 1. (Color online) A sketch of the finite-temperature crossover phase diagram close to the quantum critical point. Crossover lines $T \sim |h-h_c|^{\nu z}$ separating the semiclassical regions from the quantum critical region are shown. The latter is traversed by the system during the quench in a time t_{QC}.

production of defects by generalizing the scaling theory to open critical system and by formulating a quantum kinetic-equation approach for the adiabatic dynamics across the quantum critical region. We found that, at weak coupling and for not too slow quenches the density of excitations is universal also in the presence of an external bath. In this paper we extend the results presented in Ref. 34 and provide a detailed derivation of the kinetic equations and of the scaling laws.

The paper is organized as follows. We first derive qualitatively the scaling laws obeyed by both the density of defects and of energy generated in a quantum quench across a generic quantum critical point in the presence of a bath (Sec. II). We then address a specific one-dimensional model possessing a quantum critical point: the *XY* spin chain in transverse magnetic field. To model the thermal reservoir, the system is coupled to a set of bosonic degrees of freedom, as in the spin-boson model. Baths are chosen with power-law spectral density and are locally coupled to strings of neighboring spins. The model, a generalization of the one studied in Ref. 34, is discussed in Sec. III. For this model, we derive a kinetic equation by means of the Keldysh technique (Sec. IV) which allows us to compute the density of defects. In Sec. V we discuss the spectrum of relaxation times needed for a comparison with the scaling approach. The density of defects and of excitation generated in a quench, and a comparison with the scaling laws is presented in Sec. VI. Finally in Sec. VII we summarize our conclusions.

II. SCALING ANALYSIS

In this section we discuss the scaling laws obeyed by the density of excitations[34] and by the energy density following a linear quench of a control parameter h from an initial value h_i to a final one h_f, through a second-order quantum critical point at h_c. The system is kept, during the entire dynamics, in contact with a bath at temperature T. In the $h-T$ plane, the adiabatic quench is described by the horizontal line shown in Fig. 1. For adiabatic quenches occurring at zero temperature, the system stops following the external drive adiabatically and can be considered as frozen around the quantum critical point. This happens roughly when the time it takes to reach and cross the quantum critical point becomes comparable to the internal time scale (the inverse gap $\Delta(h) \simeq |h-h_c|^{-\nu z}$). The determination of this crossover point is the fundamental ingredient determining the scaling of the density of excitations in the case of unitary evolution.[13,14] In the case of a finite temperature quench there is a new important time scale which enters the problem, the time at which the system enters (and eventually leaves) the quantum critical region (see Fig. 1). Initially the system is in equilibrium with the bath at a low temperature $[T \ll \Delta(h_i)]$ and the behavior is, to a large extent, similar to the zero-temperature case. In the quantum critical region,[35] characterized by the crossover temperature $T \sim |h-h_c|^{\nu z}$, the gap is much smaller than the temperature itself. One can therefore expect that during the interval the system spends in the quantum critical region, a number of excitations will be produced by the presence of the environment. Interestingly also this contribution to the defect production obeys a scaling law.[36]

We now proceed with the derivation of the scaling laws. In the rest of the paper we will consider the density $\mathcal{E}$ and the energy density E of excitations, defined, respectively,

$$\mathcal{E} = \int \frac{d^d k}{(2\pi)^d} \mathcal{P}_k, \tag{1}$$

$$E = \int \frac{d^d k}{(2\pi)^d} E_k \mathcal{P}_k, \tag{2}$$

where $\mathcal{P}_k$ is the population of the excitation with quantum number k, E_k the energy spectrum at h_f, and d is the dimensionality of the quantum system.

The first assumption we make consists in separating the density of excitations/energy at the end of the quench in the sum of two (coherent and incoherent) contributions

$$\mathcal{E} \simeq \mathcal{E}_{\rm coh} + \mathcal{E}_{\rm inc}, \tag{3}$$

$$E \simeq E_{\rm coh} + E_{\rm inc}. \tag{4}$$

In the previous equation, $E_{\rm coh}$ ($\mathcal{E}_{\rm coh}$) is the density of energy (excitations) of the system produced coherently in the absence of the bath; the incoherent contribution $E_{\rm inc}$ ($\mathcal{E}_{\rm inc}$) arises instead from the bath/system interaction. The separation of a coherent and an incoherent contribution, Eqs. (3) and (4), requires weak coupling α between the system and the bath. Evidence for the validity of this assumption will be shown below [see Eqs. (10) and (11)].

In the absence of an environment, the density of excitations was shown to obey the KZ scaling[13,14]

$$\mathcal{E}_{\rm coh} = \mathcal{E}_{\rm KZ} \propto v^{d\nu/(z\nu+1)}. \tag{5}$$

In order to obtain a similar relation for the energy density in Eq. (30), additional information on E_k at h_f is needed. Thus, the scaling of this quantity depends on the details of the system at the end of the quench. A simple scaling law can be obtained only in specific situations, e.g., for quenches halted at the critical point $h_f = h_c$, where $E_k \propto k^z$. By using techniques similar to those employed in Ref. 14 one obtains

$$E_{\mathrm{coh}} \propto v^{\nu(d+z)/(z\nu+1)}. \tag{6}$$

Let us now derive a scaling law for the incoherent contributions $\mathcal{E}_{\mathrm{inc}}$ and E_{inc}. To this end it is convenient to divide the quench in three steps (see Fig. 1). Initially the system is in the so-called low-temperature region at $T \ll \Delta$. Here the relatively high-energy gap suppresses thermal excitation and the system remains in the ground state. Close to the critical point, the system passes through the quantum critical region; thermal excitations are unavoidably created because of the relatively high temperature $T \gg \Delta$. As we shall see below, the density of excitations generated in this region is a universal function of the velocity of the quench and of the temperature as long as only the low-energy details of the system spectrum matter. On the contrary, the bath-induced relaxation occurring once the system leaves the quantum critical region, entering the other semiclassical region ($T \ll \Delta$), depends on the details of the energy spectrum; hence the relaxation toward an asymptotic thermal state at temperature T is not expected to be universal if the final h_f is far off the critical point h_c. In our analysis below, we will neglect the effects of this nonuniversal relaxation. We are therefore assuming that the time elapsed between the moment when the critical region is left and when the quench is stopped (and the measurement of the density of excitations/energy is made) is short as compared to the typical relaxation times in the semiclassical region. In Sec. VI, we will further comment on this point for the specific case of the quantum XY chain, showing that the scenario just depicted holds for a wide range of h_f and v. The dynamics of the probability $\mathcal{P}_k$ of exciting the mode k can be described, inside the quantum critical region, in terms of a phenomenological rate equation

$$\frac{d}{dt}\mathcal{P}_k = -\frac{1}{\tau}[\mathcal{P}_k - \mathcal{P}_k^{th}(h_c)], \tag{7}$$

where $\mathcal{P}_k^{th}(h_c)$ is the critical thermal equilibrium distribution and τ^{-1} is the relaxation rate, $\tau^{-1} \propto \alpha T^{\theta}$. As shown in Sec. V and in the Appendix, θ can be related to characteristics of the bath and to the critical indices of the phase transition [see Eq. (A5)]. From the relation $T \sim \Delta \sim |h - h_c|^{\nu z}$ we deduce the time spent inside the quantum critical region as

$$t_{QC} = 2T^{1/\nu z} v^{-1}.$$

A direct integration of Eq. (7) gives, for the thermal excitation created in the quantum critical region, $\mathcal{P}_k \sim (1 - e^{-t_{QC}/\tau})\mathcal{P}_k^{th}(h_c)$. Finally, integrating the latter over all k modes we get

$$\mathcal{E}_{\mathrm{inc}} \propto (1 - e^{-t_{QC}/\tau}) \int dE\, E^{d/z-1} \mathcal{P}_k^{th}(h_c), \tag{8}$$

where we used the scaling of the excitation energy $E \propto k^z$. For the density of energy, a similar relation holds for quenches halted at the critical point

$$E_{\mathrm{inc}} \propto (1 - e^{-t_{QC}/(2\tau)}) \int dE\, E^{d/z} \mathcal{P}_k^{th}(h_c), \tag{9}$$

where $t_{QC}/2$ is due to the fact that in this case only half of the quantum critical region is crossed. Finally, since the thermal distribution is a function of E/T, a simple change in variable gives the required results

$$\mathcal{E}_{\mathrm{inc}} \propto \alpha v^{-1} T^{\theta + (d\nu + 1/\nu z)}, \tag{10}$$

$$E_{\mathrm{inc}} \propto \alpha v^{-1} T^{\theta + [(d+z)\nu + 1/\nu z]}, \tag{11}$$

valid in the limit $T^{1/\nu z} \ll v\tau$. Equations (10) and (11) together with Eqs. (5) and (6) give, through the assumptions Eqs. (3) and (4), the general scaling law for the quench dynamics of open systems. The different scaling of the two contributions with respect to the velocity v implies that for slow quenches $v < v_{\mathrm{cross}}$, the incoherent mechanism of excitation dominates over the coherent one and vice versa for $v > v_{\mathrm{cross}}$. The crossover velocity can be deduced by equating $\mathcal{E}_{\mathrm{inc}} \simeq \mathcal{E}_{\mathrm{coh}}$ and $E_{\mathrm{inc}} \simeq E_{\mathrm{coh}}$ yielding

$$v_{\mathrm{cross}}^{\mathcal{E}} \propto \alpha^{[\nu z + 1/\nu(z+d)+1]} T^{\{1+[(\theta-1)\nu z/\nu(z+d)+1]\}[1+(1/\nu z)]}, \tag{12}$$

$$v_{\mathrm{cross}}^{E} \propto \alpha^{[\nu z + 1/\nu(2z+d)+1]} T^{\{1+[(\theta-1)\nu z/\nu(2z+d)+1]\}[1+(1/\nu z)]}. \tag{13}$$

III. QUANTUM XY MODEL WITH THERMAL RESERVOIR

The scaling laws derived above will be tested against a specific model; an XY chain coupled to a set of bosonic baths. The Hamiltonian of the XY chain is defined as

$$H_S = -\frac{1}{2}\sum_j^N \left(\frac{1+\gamma}{2}\sigma_j^x \sigma_{j+1}^x + \frac{1-\gamma}{2}\sigma_j^y \sigma_{j+1}^y + h\sigma_j^z \right). \tag{14}$$

Here N is the number of sites ($\sigma^{x,y,z}$ are Pauli matrices). Each spin is coupled to its neighbors by anisotropic Ising-type interactions and subject to a transverse magnetic field h (the couplings are expressed in units of the exchange energy). In the thermodynamic limit $N \to \infty$, a quantum phase transition at $h_c = 1$ separates a paramagnetic phase ($h > 1$) from a ferromagnetic phase ($h < 1$) where the Z_2 symmetry is spontaneously broken and a magnetic order along $\vec{x}$ appears, $\langle \sigma^x \rangle \neq 0$.

The spin Hamiltonian (14) can be diagonalized by using the Jordan-Wigner transformation[37] to map the spins into spinless fermions c_j, thus obtaining in momentum space

$$H_S = \sum_{k>0} \Psi_k^{\dagger} \hat{\mathcal{H}}_k \Psi_k$$

$$\hat{\mathcal{H}}_k = -(\cos k + h)\hat{\tau}_z + \gamma \sin k \hat{\tau}_y, \tag{15}$$

where $\Psi_k^{\dagger} = (c_k^{\dagger}\ c_{-k})$ are Nambu spinors and $\hat{\tau}$ are Pauli matrices in Nambu space. Finally, a Bogoliubov rotation diagonalizes the Hamiltonian $H_S = \Sigma_{k>0} \Lambda_k (\eta_k^{\dagger}\eta_k - \eta_{-k}\eta_{-k}^{\dagger})$, where

$$\Lambda_k = \sqrt{(\cos k + h)^2 + (\gamma \sin k)^2}, \tag{16}$$

is the quasiparticle energy spectrum. At $h = h_c$ the spectrum becomes gapless with a linear dispersion relation $\Lambda_k \propto \pi - k$; accordingly, the critical indexes of the model are $\nu = z = 1$.

The spins are also locally coupled to a set of N/l bosonic baths

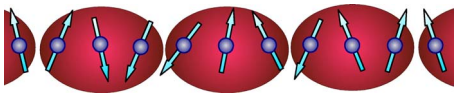

FIG. 2. (Color online) A cartoon of the spins-baths coupling [Eq. (17)] for $l=3$, i.e., each bath coupled to three spins.

$$H_{\rm int} = -\frac{1}{2}\sum_{j=0}^{N/l-1}\left(\sum_{r=0}^{l-1}\sigma^z_{jl+r}\right)X_j, \tag{17}$$

where $X_j=\Sigma_\beta\lambda_\beta(b^\dagger_{\beta,j}+b_{-\beta,j})$ and $b^\dagger_{\beta,j}$ $(b_{\beta,j})$ are the creation (annihilation) operators of the jth bosonic bath. The total Hamiltonian reads

$$H = H_S + H_{\rm int} + H_B, \tag{18}$$

where $H_B=\Sigma_{j,\beta}\omega_\beta b^\dagger_{\beta j}b_{\beta j}$. The spectral density of the baths $J(\omega)=\Sigma_\beta\lambda^2_\beta\delta(\omega-\omega_\beta)$ is

$$J(\omega) = 2\alpha\omega^s e^{-\omega/\omega_c}\theta(\omega), \tag{19}$$

where α is the system/bath coupling, ω_c is a high-energy cutoff and $\theta(s)$ is the step function.[38] According to Eq. (17), each bath interacts with a string of l adjacent spins (see Fig. 2). The model presented above generalizes the one considered in Ref. 34, where the spins were individually coupled $(l=1)$ to Ohmic baths $(s=1)$.

Local dissipation is present, for instance, in arrays of Josephson (or quantum dot) qubits (see Ref. 39 for a proposal of a Josephson junctions realization of the Ising model). In this case fluctuating charged impurities close to the junction are the major source of decoherence.[40] This environment is local, being, at most, correlated over a small number of qubits. Spin models with on-site dissipation have been considered in the recent literature in the context of dissipation-driven quantum phase transitions[41] (see also Ref. 42 for a recent proposal of a cold atom realization of the dissipative Ising model).

In momentum space $b_{\beta,q}=\frac{1}{\sqrt{N/l}}\Sigma_{j=0}^{N/l-1}\exp(-iqj)b_{\beta,j}$ with $q=\frac{2m\pi}{N/l}$ and after the Jordan-Wigner transformation we get

$$H_{\rm int} = -\frac{1}{\sqrt{N}}\sum_k\sum_q F(q)\Psi^\dagger_k\hat{\tau}^z\Psi_{k+(q/l)}X_q, \tag{20}$$

where $F(q)=1/\sqrt{l}\Sigma_{r=0}^{l-1}\exp(-irq/l)$. For $l=1$, each spin interacts with a different bath and according to Eq. (20) all k modes are coupled (i.e., transitions $k\leftrightarrow k'$, $\forall k,k'$ are induced). In the opposite case of $l=N$, (just one bath for the whole system) no transition between different k is allowed. In the intermediate case, each mode interacts with the other modes in an interval of width π/l.

It is important to notice that correlations between baths over a finite distance would not change, qualitatively, our picture as long as we focus on the critical properties of the model. Indeed, near criticality, the divergence of the correlation length makes the details of the bath correlations over microscopic distances unimportant. For the same reason, as long as one is interested in the low-T properties of the bath, the specific value of l is not relevant provided $l/N\to 0$ in the thermodynamic limit. Specifically, for all values of l such that $T\ll(\frac{1}{l})^z$, the same dissipative dynamics is obtained, since transitions with large Δk (and hence large energy) are thermally suppressed (we used $E\propto k^z$ at a fixed T). In this regime, therefore, the system cannot resolve the microscopic details of different system-bath couplings (i.e., whether $l=1,2,3,\ldots$). In the following, we thus focus on the case $l=1$: specific high-temperature and noncritical behaviors for different l could be easily investigated within the same scheme considered below. Only if $l=N$ the dynamics of the system changes qualitatively.

IV. KINETIC EQUATION

In this section we derive a kinetic equation for the Green's function of the Jordan-Wigner fermions within the Keldysh formalism. In terms of this Green's function, we then calculate both the excitation and the energy densities, Eqs. (1) and (2). Our analysis in terms of a kinetic equation will provide support for the scaling laws obtained above, Eqs. (10) and (11), while allowing us to study the nonuniversal dynamics beyond the limit of applicability of the scaling approach.

The fermionic Keldysh Green's function is a matrix in Nambu space defined by

$$[G_k(t_1,t_2)]_{i,j} \equiv -i\langle\mathcal{T}_\gamma\Psi_{ki}(t_1)\Psi^\dagger_{kj}(t_2)\rangle, \tag{21}$$

where γ is the Keldysh contour. In the following we neglect the initial correlations between system and bath.[43] Hence γ consists of just a forward and backward branch on the real time axis.

The starting point of our derivation is the Dyson's equation in its integrodifferential form

$$[i\partial_{t_1}-\hat{\mathcal{H}}_k(t_1)]G_k(t_1,t_2) = \delta(t_1-t_2) + \int_\gamma d\bar{t}\Sigma_k(t_1,\bar{t})G_k(\bar{t},t_2) \tag{22}$$

and an analogous one obtained by differentiation with respect t_2. Here Σ_k is the self-energy associated to the interaction of the system with the bath. In order to compute the energy and excitations densities, we need to find the equal-time statistical Green's functions. The latter are defined as

$$[G^<_k(t_1,t_2)]_{i,j} \doteq i\langle\Psi^\dagger_{k,j}(t_2)\Psi_{k,i}(t_1)\rangle, \tag{23}$$

$$[G^>_k(t_1,t_2)]_{i,j} \doteq -i\langle\Psi_{ki}(t_1)\Psi^\dagger_{kj}(t_2)\rangle. \tag{24}$$

An equation for these correlators can be obtained from Eq. (22) by using standard techniques.[44,45] For the equal-time Green's function $G^<_k(t,t)$ we obtain

$$i\partial_t G^<_k = [\hat{\mathcal{H}}_k, G^<_k] + \Sigma^>_k\cdot G^<_k - \Sigma^<_k\cdot G^>_k + G^<_k\cdot\Sigma^>_k - G^>_k\cdot\Sigma^<_k, \tag{25}$$

where the dots indicate the convolution

$$\Sigma^>_k\cdot G^<_k \doteq \int_0^t d\bar{t}\Sigma^>_k(t,\bar{t})G^<_k(\bar{t},t).$$

In order to proceed with the solution of Eq. (25), it is now important to discuss the approximations we make for the self-energy. Let us first notice that long-time correlations in-

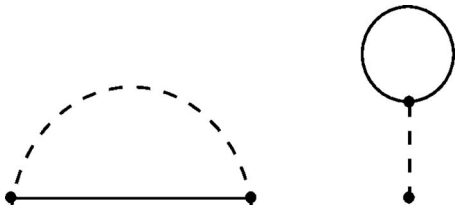

FIG. 3. Lowest-order diagrams contributing to the self-consistent Born approximation: dashed lines correspond to the non-interacting bath Green's function $g \doteq -i\langle \mathcal{T}_\gamma X_q(t_1) X_q(t_2)\rangle$ while solid lines to the interacting system Green function G. (a) corresponds to $\Sigma_k(t_1,t_2)=\frac{i}{N}\Sigma_q g_{k-q}(t_1,t_2)\tau^z G_q(t_1,t_2)\tau^z$, while (b) is the polaronic shift contribution $\Sigma_k^\delta(t_1,t_2)=-\frac{i}{N}\delta(t_1,t_2)\tau^z\int_\gamma d\bar{t} g(t_1,\bar{t})\Sigma_q \mathrm{Tr}[\tau^z G_q(\bar{t},\bar{t})]$

duced by the bath may change the universality class of the transition by renormalizing the low-energy spectrum of the system.[46] We will not consider this case here. Therefore, we assume that the bosons have a nonzero inverse lifetime $\Gamma \ll T$ which provides a natural cut-off time for the bath correlation functions. Within this assumption it is now possible to describe the kinetics of the system using a Markov approximation together with a self-consistent Born approximation. The latter is justified for weak system/bath coupling ($\alpha \ll 1$) and is represented diagrammatically in Fig. 3(a). We will neglect the tadpole diagram 3(b), which represents just a small shift in the energy levels.

We now use the interaction picture

$$\tilde{G}_k(t_1,t_2) \doteq \hat{\mathcal{U}}_k^\dagger(t_1) G_k(t_1,t_2)\hat{\mathcal{U}}_k(t_2),$$

where $\hat{\mathcal{U}}_k(t_0,t)$ is the evolution operator satisfying $i\partial_t\hat{\mathcal{U}}_k = \hat{\mathcal{H}}_k(t)\hat{\mathcal{U}}_k$. It is evident that, within our assumptions, the evolution of $\tilde{G}_k$ can be considered slow as compared to that of the bath correlators appearing in the self-energies. Using this separation of time scales, it is possible to implement the Markov approximation and transform the general integrodifferential kinetic equation into a simple differential equation. We then obtain, for the case in which each spin is coupled to its own bath ($l=1$), the kinetic equation

$$\partial_t G_k^< + i[\mathcal{H}_k, G_k^<] = \frac{1}{N}\sum_q \tau^z(\mathbf{1}+iG_q^<)\hat{D}_{qk}G_k^< + \tau^z G_q^<\hat{D}_{kq}^\dagger(\mathbf{1} + iG_k^<) + \mathrm{H.c.}, \tag{26}$$

where

$$\hat{D}_{qk} = i\int_0^\infty ds\, g^>(s)\hat{\mathcal{U}}_q^\dagger(t,t-s)\hat{\tau}^z\hat{\mathcal{U}}_k(t,t-s), \tag{27}$$

$g^>(t) = -i\langle X_q(t)X_q(0)\rangle$. The left-hand side of Eq. (26) represents the free evolution term, while the right-hand side describes the scattering between the k modes mediated by the bath degrees of freedom.

In the eigenbasis of the Hamiltonian $\hat{\mathcal{H}}_k$, the Green's function can be parametrized as

$$-iG_k^< = \begin{pmatrix} \mathcal{P}_k & \mathcal{C}_k \\ \mathcal{C}_k^* & 1-\mathcal{P}_k \end{pmatrix}, \tag{28}$$

where $\mathcal{P}_k = \langle \eta_k^\dagger \eta_k\rangle$ is the population of the excited mode k and $\mathcal{C}_k = \langle \eta_{-k}\eta_k\rangle$ can be regarded as a "coherence" term.[47,48] In the static case, where the evolution operator is $\hat{\mathcal{U}}_k = \exp(-i\hat{\mathcal{H}}_k t)$, the stationary solution of the kinetic equation (26) is correctly the thermal equilibrium one: $\mathcal{C}_k = \mathcal{C}_k^{th} = 0$ and $\mathcal{P}_k = \mathcal{P}_k^{th} = (e^{\Lambda_k/k_BT}+1)^{-1}$ (the Fermi function). Once the solution of the kinetic equation (26) is obtained, the density of excitations and energy produced during the quench can be expressed as

$$\mathcal{E} = \frac{1}{N}\sum_{k>0}\mathcal{P}_k, \tag{29}$$

$$E = \frac{1}{N}\sum_{k>0}\Lambda_k\mathcal{P}_k. \tag{30}$$

We conclude this section by commenting on a useful approximation to evaluate numerically the kernel of $\hat{D}_{qk}$, Eq. (27). It consists in approximating the evolution operator $\hat{\mathcal{U}}_k$ appearing in $\hat{D}_{qk}$ with $\hat{\mathcal{U}}_k(t,t-s) \simeq \exp(i\hat{\mathcal{H}}_k(t)s)$, thus obtaining

$$\hat{D}_{qk} \simeq i\int_0^\infty ds\, g^>(s)\exp(-i\hat{\mathcal{H}}_k(t)s)\hat{\tau}^z\exp(i\hat{\mathcal{H}}_k(t)s). \tag{31}$$

This is consistent with the separation of time scales mentioned above (Markov approximation). In fact, if the quench is slow on the time-scale characteristic of the bath, the correlation function $g^>(s)$ can be considered as strongly peaked at $s=0$. Hence, for the bath dynamics the system can be considered "frozen" at the instantaneous value of $h(t)$ and, consistently, its evolution operator is the exponential of the Hamiltonian.

V. RELAXATION TIME

In order to make further progress in understanding the quench dynamics of the system, we will first extract from the kinetic equation the characteristic relaxation time for the populations of the excitations $\mathcal{P}_k$ [see Eq. (28)] as a function of the magnetic field h and the temperature T. For this purpose, it is sufficient to consider only the diagonal elements of Eq. (28). This is equivalent to the so-called "secular approximation" for the master equation,[48] which is valid for weak couplings ($\alpha \ll 1$ in the present case). The set of $N/2$ (only $N/2$ modes are independent) nonlinear equations (26) can be linearized near the thermal equilibrium fixed point in order to analyze the asymptotic relaxation. With the vector notation $\underline{\delta\mathcal{P}} = (\delta\mathcal{P}_1, \delta\mathcal{P}_2, \ldots, \delta\mathcal{P}_{N/2})^{\mathrm{tr}}$, where $\delta\mathcal{P}_k = \mathcal{P}_k - \mathcal{P}_k^{th}$, we obtain

$$\frac{d}{dt}\delta\underline{\mathcal{P}} = -\mathcal{R}\cdot\delta\underline{\mathcal{P}}, \tag{32}$$

where nonlinear terms in $\delta\mathcal{P}_k$ have been neglected. The diagonal and off-diagonal elements of the $N/2\times N/2$ matrix $\mathcal{R}$ are

$$\begin{aligned}\mathcal{R}_{kk} = \frac{2}{N}\sum_{q>0,q\neq k}\{&\mathcal{G}_q^{th}[1-\cos(\theta_k+\theta_q)]g[-\Lambda_k-\Lambda_q]+\mathcal{G}_q^{th}[1\\&+\cos(\theta_k+\theta_q)]g[\Lambda_k-\Lambda_q]+\mathcal{P}_q^{th}[1-\cos(\theta_k+\theta_q)]g[\Lambda_k\\&+\Lambda_q]+\mathcal{P}_q^{th}[1+\cos(\theta_k+\theta_q)]g[-\Lambda_k+\Lambda_q]\}\\&+\frac{2}{N}4\sin^2\theta_k[\mathcal{G}_k^{th}g(-2\Lambda_k)+\mathcal{P}_k^{th}g(2\Lambda_k)],\end{aligned} \tag{33}$$

$$\begin{aligned}\mathcal{R}_{kq} = \frac{2}{N}\{&-\mathcal{G}_k^{th}[1+\cos(\theta_k+\theta_q)]g[-\Lambda_k+\Lambda_q]+\mathcal{G}_q^{th}[1\\&-\cos(\theta_k+\theta_q)]g[-\Lambda_k-\Lambda_q]-\mathcal{P}_q^{th}[1+\cos(\theta_k\\&+\theta_q)]g[\Lambda_k-\Lambda_q]+\mathcal{P}_q^{th}[1-\cos(\theta_k+\theta_q)]g[\Lambda_k+\Lambda_q]\},\end{aligned} \tag{34}$$

where $g[E]=\pi[J(E)-J(-E)]\frac{\exp(\beta E)}{\exp(\beta E)-1}$ is the real part of the Laplace transform of the bath correlation function [we neglect the imaginary part since it gives a renormalization contribution that is negligible in the weak-coupling limit $\alpha\to 0$ (Ref. 48)], $\mathcal{G}_k^{th}$ is the thermal equilibrium value of the population of the ground state of mode k, $\mathcal{G}_k^{th}=1-\mathcal{P}_k^{th}$, and

$$\theta_k = \arccos -\frac{(\cos k+h)}{\Lambda_k}. \tag{35}$$

The eigenvalues of $\mathcal{R}$, $\{\lambda_i\}$, are the characteristic relaxation rates of the long-time dynamics. Hence, the solution of Eq. (32) for each population would be a linear combination containing all the characteristic relaxation times

$$\delta\mathcal{P}_k = \sum_j r_{kj}e^{-\lambda_j t}.$$

At long times $t\gg(\min_j\lambda_j)^{-1}\doteq\tau$, all modes relax with the same relaxation time τ. In the following, we first analyze the longest relaxation time τ, extending the results presented in Ref. 34; we then study the structure of the entire spectrum of relaxation times.

In Fig. 4 we show the general behavior of τ in the finite-temperature phase diagram, calculated by numerically diagonalizing the matrix $\mathcal{R}$. As $T\to 0$, τ diverges and close to the critical point, two different behaviors are found in the semiclassical regions and in the quantum critical region (see also Fig. 1)

$$\tau^{-1}\propto\begin{cases}T^{1+s} & T\gg\Delta\\ e^{-\Delta/T} & T\ll\Delta\end{cases}. \tag{36}$$

These relations extend the results obtained for the relaxation rate in Ref. 34 to the generic case of non-Ohmic baths and give the exponent θ as $\theta=1+s$.

An analytic expression for the power-law scaling inside the quantum critical region can be obtained by approximating the smallest eigenvalue of $\mathcal{R}$ with the smallest diagonal element. This is justified by the fact that the off-diagonal elements are of the order $O(1/N)$ [see Eq. (34)]. For $h=h_c=1$, considering the gapless mode $k=\pi$, we have from Eq. (33) in the continuum limit

$$\begin{aligned}\tau_{\rm diag}^{-1}\doteq\mathcal{R}_{\pi\pi} &= \frac{2}{\pi}\int_0^\pi dq(\mathcal{G}_q^{th}g[-\Lambda_q]+\mathcal{P}_q^{th}g[\Lambda_q])\\&=4\alpha\int_0^\pi dq\frac{\Lambda_q^s}{\sinh(\Lambda_q/T)}\simeq 8\alpha(1-2^{-1-s})\Gamma(1+s)\zeta(1+s)\\&\times(\gamma/T)^{-1-s},\end{aligned} \tag{37}$$

where Γ and ζ are the Gamma and the zeta functions, and we used the critical dispersion relation $\Lambda_q\simeq\gamma(\pi-q)$ obtained by linearizing Eq. (16) around the gapless point $k=\pi$ (we extended the integration to $-\infty$ since at low temperature only the low-energy modes contribute to the integral). Figure 5 demonstrates that the analytical expression in Eq. (37) agrees very well with the numerical solution (obtained by diagonalizing $\mathcal{R}$) especially at low temperature.

As we have shown in Fig. 5, inside the quantum critical region the exponent θ is universal within the range of anisotropy $0<\gamma\leq 1$ where the system belongs to the Ising univer-

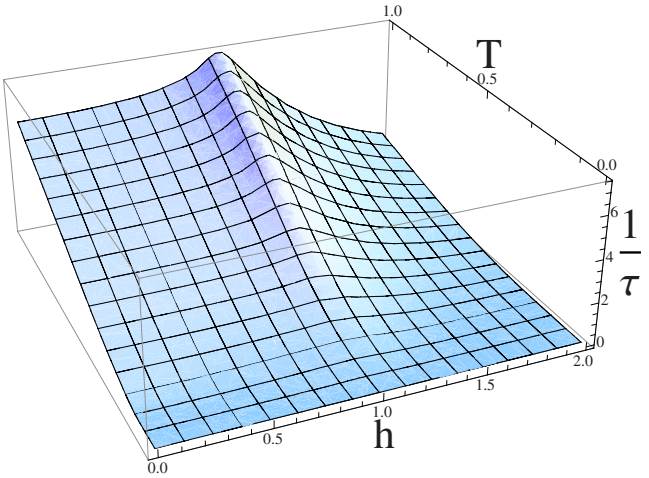

FIG. 4. (Color online) Relaxation rate $1/\tau$ as a function of T and h for $N=400$ (here $\gamma=1$, and $s=1$).

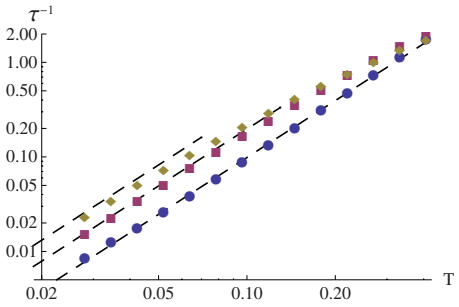

FIG. 5. (Color online) Relaxation rate $1/\tau$ as a function of T obtained from the exact diagonalization of $\mathcal{R}$ (symbols) and the approximation in Eq. (37) (dashed lines). Lines are relative to $\gamma=0.3$, 0.5, and 1 (from top to bottom) and $h=1$, $s=1$.

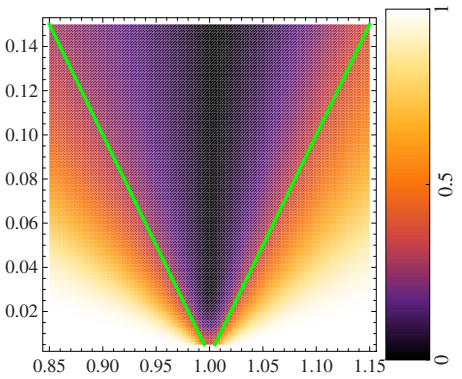

FIG. 6. (Color online) Ising model ($\gamma=1$) with Ohmic baths ($s=1$). Relative gap between the two longest relaxation times $(\lambda_2^{-1}-\lambda_1^{-1})/\lambda_1^{-1}$ ($\lambda_{1,2}$ being the two lowest eigenvalues of $\mathcal{R}$) as a function of T and h; crossover lines $T=\Delta=|h-1|$ are plotted for comparison.

sality class. This suggests a relation between θ and the critical indexes of the quantum phase transition. Indeed, it can be shown, within the Fermi golden rule (see Appendix), that for a generic system coupled to a bosonic bath, the following expression holds inside the quantum critical region:

$$\tau^{-1} \propto T^{s+d/z}. \tag{38}$$

An important feature of the relaxation dynamics can be extracted by analyzing the spectrum of the eigenvalues $\{\lambda_j\}$ of $\mathcal{R}$. We find that in the semiclassical regions $T \ll \Delta$ the smallest eigenvalue of $\mathcal{R}$ is separated from the rest of the spectrum by a gap (even in the $N \to \infty$ limit). On the contrary, inside the quantum critical region, such eigenvalue merges with the rest of the spectrum. This can be quantified by the relative gap in the spectrum of relaxation times that is identified by $(\lambda_2^{-1}-\lambda_1^{-1})/\lambda_1^{-1}$, $\lambda_{1,2}$ being the lowest eigenvalues of $\mathcal{R}$ (see Fig. 6). This result indicates that while the exponential divergence of the relaxation time $\tau \propto \exp\{\Delta/T\}$ in the semiclassical regions is due to an isolated eigenvalue, the long-time behavior in the quantum critical region is, instead, built up by a continuum of eigenvalues contributing to the $\tau^{-1} \propto T^{s+1}$ scaling.

VI. ADIABATIC QUENCHES

Equipped with the kinetic equation and the knowledge of the scaling of the relaxation times, we now analyze the quench dynamics of the model in Eq. (18) by numerically solving the kinetic equation (26). The system is initialized at $h_i \gg h_c$ in equilibrium with the bath at a fixed temperature $T \ll \Delta(h_i)$ and the transverse field is then ramped linearly $h(t)=h_i-vt$ down to a final value h_f (the bath temperature is kept fixed).

In Fig. 7 we plot the density of excitations as a function of the quench velocity for different system sizes (a similar behavior is obtained for the density of energy). Additionally, we considered separately the coherent ($\mathcal{E}_{\rm coh}$) and incoherent contribution ($\mathcal{E}_{\rm inc}$) to the final density of excitations. The first one is obtained by integrating the kinetic equation for $\alpha=0$, i.e., no coupling with the bath. The incoherent term is due to

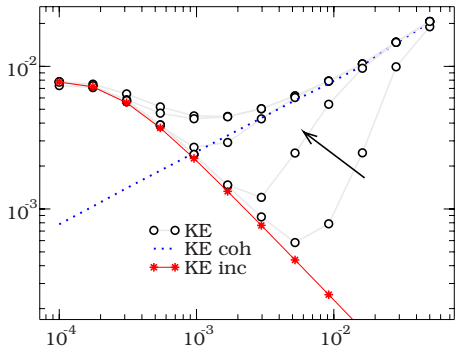

FIG. 7. (Color online) Density of excitation $\mathcal{E}$ (circles) versus quench velocity for different system sizes $N=26$, 50, 100, 200, 400, and 800 from bottom to top, according to the arrow; the points corresponding to $N=800$ and $N=400$ are indistinguishable. Parameters are set to $\alpha=0.01$, $T=0.1$ $\gamma=1$ and $s=1$ and the quench is halted at $h_f=0.8$. Dotted line is the coherent contribution $\mathcal{E}_{\rm coh}$ obtained for $\alpha=0$ and stars represent the incoherent contribution $\mathcal{E}_{\rm inc}$ due to thermal excitation (see text); both curves are relative to $N=800$; for $\mathcal{E}_{\rm inc}$ the same curve is obtained already at $N \sim 30$.

thermal excitations created by the bath and is obtained by integrating the kinetic equation ignoring the unitary evolution term $i[\hat{\mathcal{H}}_k, \hat{G}_k^<]$ responsible for the coherent excitation process.

In order to understand the two excitation mechanisms we analyze directly the dynamics of the populations $\mathcal{P}_k$. From the results shown in Fig. 8 (left), it emerges that excitations are generated close to the critical point and, subsequently,

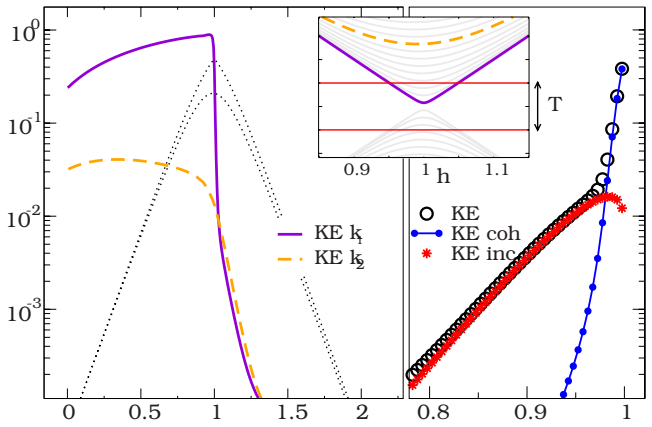

FIG. 8. (Color online) Populations of the excited states $\mathcal{P}_k$ for $N=400$, $v=0.0017$, and the same parameter values of Fig. 7. Left: dynamics of two low-energy modes $k_1 \sim \pi$ (solid line) and $k_2 \sim 0.9\pi$ (dashed line) as a function of $h(t)$ obtained by solving the kinetic equation (instantaneous thermal equilibrium values are plotted for reference as dotted lines). The inset shows the energy levels near the critical point and the scale of temperature; marked levels refer to k_1 and k_2. The energy gap closes at $k=\pi$. Right: distribution of $\mathcal{P}_k$ as a function of k at $h(t)=1$. Stars represent the excitations created incoherently and triangles represent the excitations produced coherently when there is no coupling to the bath. The two excitation mechanisms act on different energy scales: the lowest energy modes are coherently populated, the highest ones thermally excited.

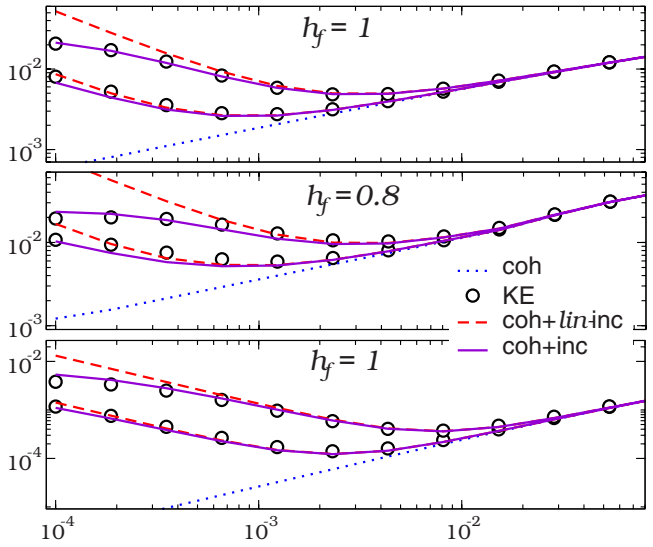

FIG. 9. (Color online) Density of energy (lowest panel) and of excitations versus quench velocity v for h_f=0.8 and 1. Parameters are set to γ=0.7, s=1.5, α=0.01, and T=0.15 or 0.1 (upper and lower curves of each panel). Circles are obtained by solving the kinetic equation; dotted lines are the coherent contributions $\mathcal{E}_{\rm coh}$ and $E_{\rm coh}$ evaluated by solving the kinetic equation for α=0; a fit gives correctly $\mathcal{E}_{\rm coh} \propto \sqrt{v}$ and $E_{\rm coh} \propto v$, consistently with the KZ scaling law for excitations [Eq. (5)] and the modified scaling we derived for the energy density [Eq. (6)]. Solid and dashed lines are Eqs. (3) and (4) using for the incoherent contributions the expressions (39) and (40) and their linearized forms Eq. (41) and Eq. (42), respectively.

relaxed out by the bath when the system is driven in the semiclassical region ($T \ll \Delta$). The density of excitation generated is the sum of the incoherent and coherent contribution, thus proving the validity of the *Ansatz* [Eqs. (3) and (4)] [see Fig. 8 (right)].

For the *XY* model, the integration of Eqs. (8) and (9) can be performed explicitly by using the critical spectrum $\Lambda_k \sim \gamma(\pi - k)$. We obtain

$$\mathcal{E}_{\rm inc} = \frac{\log 2}{2\pi\gamma} T(1 - e^{-2T/(\pi v)}), \tag{39}$$

$$E_{\rm inc} = \frac{\pi}{24\gamma} T^2(1 - e^{-T/(\pi v)}), \tag{40}$$

where the latter holds for quenches halted at $h_f = h_c$. In the previous formulas, the expression derived for τ in Eq. (37) can be used to get a fully analytical expression. Expanding the exponentials in Eqs. (39) and (40), we obtain

$$\mathcal{E}_{\rm inc} \simeq \frac{8 \log 2}{\pi} \varphi(s) \alpha \gamma^{-2-s} v^{-1} T^{3+s}, \tag{41}$$

$$E_{\rm inc} \simeq \frac{\pi}{3} \varphi(s) \alpha \gamma^{-2-s} v^{-1} T^{4+s}, \tag{42}$$

where $\varphi(s) = (1 - 2^{-1-s})\Gamma(1+s)\zeta(1+s)$. The previous relations are consistent with Eqs. (10) and (11) with $\theta = 1 + s$ (see Eq. (38)).

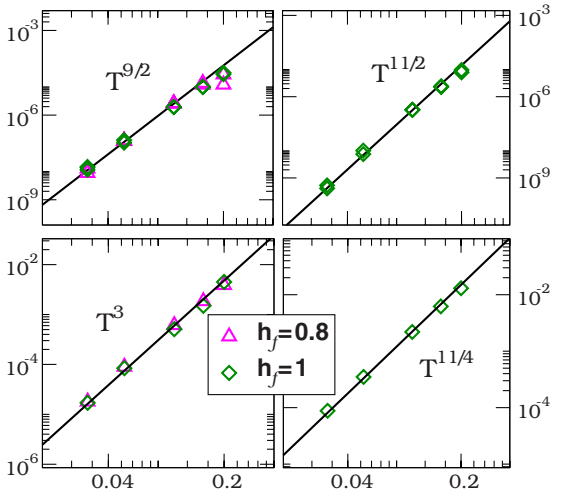

FIG. 10. (Color online) System and bath parameters are fixed as in Fig. 9. Upper panel: data collapse of $v\mathcal{E}_{\rm inc}$ and $vE_{\rm inc}$ as a function of T obtained from the kinetic equation; data refer to $10^{-3} \lesssim v \lesssim 10^{-2}$ (data relative to h_f=1 for $\mathcal{E}_{\rm inc}$ are rescaled by a factor 2, since in this case only half quantum critical region is crossed). Lower panel: scaling of $v_{\rm cross}$ is obtained equating $\mathcal{E}_{\rm inc} = \mathcal{E}_{\rm coh}$ and analogously for E. The fits confirm the scaling predicted by Eqs. (10) and (11) and Eqs. (12) and (13), that, for the specific case of s=1.5 considered, are shown in their corresponding plots.

In Fig. 9 the density of excitations and energy obtained from the solution of kinetic equation is compared with the scaling law derived in Sec. II using the specific expressions, Eqs. (39) and (40), derived above for the *XY* model. The scaling laws are found to be in good agreement with the numerical data. The results shown in Fig. 10 further confirm the scaling as a function of the temperature and the relations (12) and (13) for the crossover velocity.

Finally, we comment on the role in the final value of magnetic field h_f at which the quench is halted. The agreement with the scaling Ansatz becomes worse for decreasing h_f (see Fig. 11). This is due to the noncritical relaxation induced by the bath when the system crosses the semiclassical region after the critical point (see Fig. 1 and Fig. 8 left). At low v the time spent therein at a relative low temperature $T \ll \Delta$ is so long that the bath is able to relax the excitations created close to the critical point.

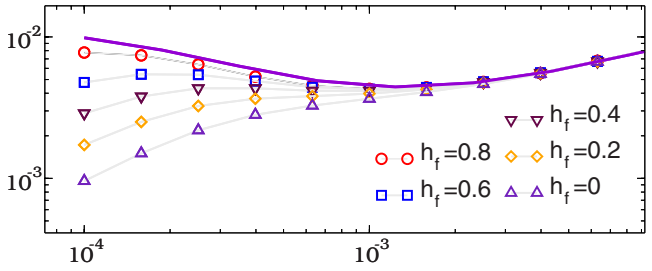

FIG. 11. (Color online) Density of excitations versus quench velocity v for h_f=0.8,0.6,0.4,0.2,0. Parameters are set to γ=1, s=1, α=0.01, and T=0.1. Upper solid line is the scaling law [Eq. (3)] using the expression (39). Decreasing the value of h_f, the crossing of the semiclassical region, after the critical point, becomes more relevant at low v and scaling no longer holds strictly.

VII. CONCLUSIONS

We have studied the dynamics of a quantum critical system coupled to a thermal reservoir and subject to an adiabatic quench across its quantum critical point. We considered the regime of weak coupling, low temperature and slow quench velocity.

The bath has two effects on the system: the first one is to create excitations inside the quantum critical region and the second to trigger the relaxation of the excitations created close to the critical point when the system is driven in the semiclassical region (see Fig. 1). While the first mechanism is universal, being entirely ruled by the critical properties of the low-energy spectrum, the latter depends on the details of the system far off the critical point. Hence, as far as the evolution is halted close to the critical point and the noncritical relaxation mechanism is negligible, universal scaling behavior is recovered. We derived scaling laws for the density of energy produced by the quench at finite temperature extending the previous results obtained for the density of excitations in Ref. 34.

To check the validity of the scaling laws, we considered the specific case of the quantum *XY* model Eq. (14) coupled locally to a set of bosonic baths, Eq. (17) (see Fig. 2). In order to study the dynamics we derived a kinetic equation within the Keldysh formalism. A detailed analysis of the characteristic relaxation time obtained from the kinetic equation was given in Sec. V. An analytic expression for the critical relaxation time was obtained in Eq. (37) and verified in Fig. 5. As shown in the Appendix, the scaling of the relaxation time as a function of the temperature is related to the critical exponents of the model [see Eq. (A5)]. Finally, we considered the quench dynamics. The kinetic equations derived allow us to study the dissipative dynamics even beyond the universal regime. We checked the scaling laws derived and their range of validity in Figs. 9 and 11.

We remark that the method described here to obtain a kinetic equation for the *XY* model, may be extended to describe the dissipative dynamics of other models that can be mapped into fermionic degrees of freedom such as other spin chains and ladders or certain $2d$ models of the Kitaev type.

ACKNOWLEDGMENTS

We acknowledge F. Guinea, V. Kravtsov, A. Polkovnikov, A. J. Leggett, R. Raimondi. F. Sols, T. Caneva, G. Carleo, and M. Schirò for fruitful discussions. D.P. acknowledges the ISTANS (Grant No. 1758) program of ESF for financial support.

APPENDIX: FERMI GOLDEN RULE FOR THE RELAXATION TIME

In this section we derive an expression for the critical relaxation time using the Fermi golden rule for a generic system interacting with a bosonic bath. Let us assume the system-bath interaction Hamiltonian to have the form $H_{\rm int}=AZ$ where A and Z are system and bath operator, respectively. Consider a quench of the system from zero temperature to a certain finite T. The transition rate for the process of thermalization in presence of the reservoir $\rho_B^{th}\otimes(|GS\rangle\langle GS|)_S\rightarrow\rho_B^{th}\otimes\rho_S^{th}$ (where B and S refer to system and bath, respectively) is

$$\frac{1}{\tau}=2\pi\sum_{f,i,k}\delta(E_f+E_k-E_i-E_{GS})P_B^{th}(E_i/T)\times P_S^{th}(E_k/T)\times|\langle k,f|H_{\rm int}|GS,i\rangle|^2, \tag{A1}$$

where i, f, and k address the bath eigenvalues and the final state of the system, respectively, and $P_{S(B)}^{th}$ are thermal weights. We rewrite the δ function as $\frac{1}{2\pi}\int_{-\infty}^{\infty}dte^{-i(E_f-E_i)t}e^{-i(E_k-E_{GS})t}$. Summing over f and i we get the bath correlation function $z(t)=\langle Z(t)Z(0)\rangle$

$$\frac{1}{\tau}=\sum_k\int_{-\infty}^{\infty}dte^{-i(E_k-E_{GS})t}z(t)P_S^{th}(E_k/T)|\langle k|A|GS\rangle|^2. \tag{A2}$$

The time integral gives the Fourier transform of the bath correlation function, that we parametrize as

$$z[E]=J(E)f(E/T). \tag{A3}$$

For instance, for a bosonic bath with spectral function $J(E)\propto E^s$ we have

$$z[E]=\begin{cases}J(E)(1+n_B(E/T)) & E>0\\ J(|E|)n_B(|E|/T) & E<0\end{cases}.$$

By integrating over the k modes (setting $E_{GS}=0$), using the critical density of states $\rho(E)\propto E^{d/z-1}$, we get

$$\frac{1}{\tau}\propto\int dE\rho(E)z[E]P_S^{th}(E/T)|A_{GS}(E)|^2,$$

where $A_{GS}(E)=\langle k(E)|A|GS\rangle$. Now, assuming that the low-energy modes (that are the relevant ones at low temperature) are coupled uniformly by the bath $A_{GS}(E)\simeq A_{GS}(0)$, we obtain

$$\frac{1}{\tau}\propto\int dE\,E^{d/z-1}J(E)f(E/T)P_S^{th}(E/T) \tag{A4}$$

and finally, using for the spectral density $J(E)\propto E^s$ and performing a change in variable to $x=E/T$, we obtain

$$\tau^{-1}\propto T^{s+d/z}. \tag{A5}$$

[1] M. Greiner, Olaf Mandel, Tilman Esslinger, Theodor W. Hänsch, and Immanuel Bloch, Nature (London) **415**, 39 (2002); M. Greiner, Olaf Mandel, Theodor W. Hänsch, and Immanuel Bloch, *ibid.* **419**, 51 (2002).
[2] T. Kinoshita, T. Wenger, and D. S. Weiss, Nature (London) **440**, 900 (2006).
[3] L. E. Sadler, J. M. Higbie, S. R. Leslie, M. Vengalattore, and D. M. Stamper-Kurn, Nature (London) **443**, 312 (2006).
[4] F. Iglói and H. Rieger, Phys. Rev. Lett. **85**, 3233 (2000); K. Sengupta, S. Powell, and S. Sachdev, Phys. Rev. A **69**, 053616 (2004); P. Calabrese and J. Cardy, Phys. Rev. Lett. **96**, 136801 (2006); P. Calabrese and J. Cardy, J. Stat. Mech.: Theory Exp. (2007) P10004; G. De Chiara, S. Montangero, and P. Calabrese, R. Fazio, J. Stat. Mech.: Theory Exp. (2006) P03001; S. Montangero, R. Fazio, P. Zoller, and G. Pupillo, Phys. Rev. A **79**, 041602(R) (2009); D. Rossini, A. Silva, G. Mussardo, and G. Santoro, Phys. Rev. Lett. **102**, 127204 (2009); P. Barmettler, M. Punk, V. Gritsev, E. Demler, and E. Altman, *ibid.* **102**, 130603 (2009).
[5] M. Rigol, V. Dunjko, V. Yurovsky, and M. Olshanii, Phys. Rev. Lett. **98**, 050405 (2007); C. Kollath, A. M. Läuchli, and E. Altman, *ibid.* **98**, 180601 (2007); S. R. Manmana, S. Wessel, R. M. Noack, and A. Muramatsu,, *ibid.* **98**, 210405 (2007); M. Cramer, C. M. Dawson, J. Eisert, and T. J. Osborne, *ibid.* **100**, 030602 (2008); T. Barthel and U. Schollwock, *ibid.* **100**, 100601 (2008); M. Eckstein and M. Kollar, *ibid.* **100**, 120404 (2008); M. A. Cazalilla, *ibid.* **97**, 156403 (2006); D. M. Gangardt and M. Pustilnik, Phys. Rev. A **77**, 041604(R) (2008).
[6] A. Polkovnikov, Phys. Rev. Lett. **101**, 220402 (2008); R. Barankov and A. Polkovnikov, arXiv:0806.2862 (unpublished).
[7] A. Silva, Phys. Rev. Lett. **101**, 120603 (2008); G. Roux, Phys. Rev. A **79**, 021608(R) (2009); A. Faribault, P. Calabrese, and J.-S. Caux, J. Stat. Mech.: Theory Exp. (2009) P03018.
[8] T. W. B. Kibble, J. Phys. A **9**, 1387 (1976); W. H. Zurek, Nature (London) **317**, 505 (1985).
[9] T. W. B. Kibble, Phys. Today **60** (9), 47 (2007).
[10] E. Farhi, Jeffrey Goldstone, Sam Gutmann, Joshua Lapan, Andrew Lundgren, and Daniel Preda, Science **292**, 472 (2001).
[11] G. E. Santoro, Roman Martonak, Erio Tosatti, and Roberto Car, Science **295**, 2427 (2002).
[12] G. E. Santoro and E. Tosatti, J. Phys. A **39**, R393 (2006).
[13] W. H. Zurek, U. Dorner, and P. Zoller, Phys. Rev. Lett. **95**, 105701 (2005).
[14] A. Polkovnikov, Phys. Rev. B **72**, 161201(R) (2005).
[15] J. Dziarmaga, Phys. Rev. Lett. **95**, 245701 (2005).
[16] B. Damski, Phys. Rev. Lett. **95**, 035701 (2005).
[17] R. Schutzhold, M. Uhlmann, Y. Xu, and U. R. Fischer, Phys. Rev. Lett. **97**, 200601 (2006).
[18] R. W. Cherng and L. S. Levitov, Phys. Rev. A **73**, 043614 (2006).
[19] B. Damski and W. H. Zurek, Phys. Rev. Lett. **99**, 130402 (2007).
[20] F. M. Cucchietti, B. Damski, J. Dziarmaga, and W. H. Zurek, Phys. Rev. A **75**, 023603 (2007).
[21] L. Cincio, J. Dziarmaga, M. M. Rams, and W. H. Zurek, Phys. Rev. A **75**, 052321 (2007).
[22] T. Caneva, R. Fazio, and G. E. Santoro, Phys. Rev. B **76**, 144427 (2007).
[23] T. Caneva, R. Fazio, and G. E. Santoro, Phys. Rev. B **78**, 104426 (2008).
[24] K. Sengupta, D. Sen, and S. Mondal, Phys. Rev. Lett. **100**, 077204 (2008).
[25] A. Polkovnikov and V. Gritsev, Nat. Phys. **4**, 477 (2008).
[26] D. Sen, K. Sengupta, and S. Mondal, Phys. Rev. Lett. **101**, 016806 (2008).
[27] U. Divakaran, V. Mukherjee, A. Dutta, and D. Sen, J. Stat. Mech.: Theory Exp. (2009) P02007.
[28] F. Pellegrini, S. Montangero, G. E. Santoro, and R. Fazio, Phys. Rev. B **77**, 140404(R) (2008).
[29] S. Deng, G. Ortiz, and L. Viola, EPL **84**, 67008 (2008).
[30] A. Fubini, G. Falci, and A. Osterloh, New J. Phys. **9**, 134 (2007).
[31] S. Mostame, G Schaller, and R. Schützhold, Phys. Rev. A **76**, 030304(R) (2007).
[32] M. H. S. Amin, C. J. S. Truncik, and D. V. Averin, arXiv:0803.1196 (unpublished).
[33] L. Cincio, J. Dziarmaga, J. Meisner, and M. M. Rams, Phys. Rev. B **79**, 094421 (2009).
[34] D. Patanè, A. Silva, L. Amico, R. Fazio, and G. E. Santoro, Phys. Rev. Lett. **101**, 175701 (2008).
[35] S. Sachdev, *Quantum Phase Transitions* (Cambridge University Press, Cambridge, 1999).
[36] Notice that depending on the characteristics of the bath, the system-bath coupling may lead to a change in universality class of the transition as a result of bath-induced long-range correlations effects. We will not address these issues here, which deserve a careful separate study. Therefore we will assume the bath correlations to be short ranged in time (Ref. 34).
[37] P. Pfeuty, Ann. Phys. **57**, 79 (1970).
[38] U. Weiss, *Quantum Dissipative Systems* (World Scientific, Singapore, 1992).
[39] L. S. Levitov, T. P. Orlando, J. B. Majer, and J. E. Mooij, arXiv:cond-mat/0108266 (unpublished).
[40] E. Paladino, L. Faoro, G. Falci, and R. Fazio, Phys. Rev. Lett. **88**, 228304 (2002).
[41] J. A. Hoyos and T. Vojta, Phys. Rev. Lett. **100**, 240601 (2008); T. Vojta and J. A. Hoyos, arXiv:0811.3754 (unpublished); J. A. Hoyos, C. Kotabage, and T. Vojta, Phys. Rev. Lett. **99**, 230601 (2007); G. Schehr and H. Rieger, J. Stat. Mech.: Theory Exp. (2008) P04012; G. Schehr and H. Rieger, Phys. Rev. Lett. **96**, 227201 (2006).
[42] P. P. Orth, I. Stanic and K. Le Hur, Phys. Rev. A **77**, 051601(R) (2008).
[43] J. Rammer and H. Smith, Rev. Mod. Phys. **58**, 323 (1986).
[44] H. Haug and A.-P. Jauho, *Quantum Kinetics in Transport and Optics of Semiconductors* (Springer, Berlin, 1996).
[45] R. van Leeuwen, N. E. Dahlen, G. Stefanucci, C.-O. Almbladh, and U. von Barth, arXiv:cond-mat/0506130 (unpublished).
[46] P. Werner, K. Volker, M. Troyer, and S. Chakravarty, Phys. Rev. Lett. **94**, 047201 (2005); P. Werner, M. Troyer, and S. Sachdev, J. Phys. Soc. Jpn. Suppl. **74**, 67 (2005).
[47] L. Landau, Phys. Z. Sowjetunion **2**, 46 (1932); C. Zener, Proc. R. Soc. London, Ser. A **137**, 696 (1932).
[48] C. Cohen-Tannoudji, J. Dupont-Roc, G. Grynberg, *Atom-photon interactions: Basic processes and applications* (Wiley-Hermann, New York, 1992).